STM JOURNALS

Journal of
Polymer & Composites

ISSN: 2321-2810 (Online)
ISSN: 2321-8525 (Print)
Volume 11, Special Issue 4, 2023
DOI (Journal): 10.37591/JoPC

http://engineeringjournals.stmjournals.in/index.php/JoPC/index

Research JoPC

TiO_2 Refined Flux Provides Significant Impact on Saw Bead Shape, Particle Size, and Hardness

Rishabh Chaturvedi[1,*], Aman Sharma[2]

Abstract

This experiment is very interested in how adding titanium dioxide powder to submerged arc welding on low alloy steel plates affects the bead geometry, grain size, and hardness. The commercial fluxes were combined with powdered titanium dioxide at varying concentrations (2.5%, 5%, 7.5%, 10%, and 12.5%). No changes were made to the welding process parameters despite the variety of welding situations. It has been shown that the inclusion of titanium dioxide significantly improves the bead geometry parameters. The optimal bead shape parameters were found at a titanium dioxide enrichment level of 5%. Titanium enrichment can be linked to amorphous ferrite formation and grain refinement in the microstructure of weld metal (WM). Increases in titanium content tend to cause the ferrite and pearlite phases' typical grain sizes to reduce. According to a phase study of WMs, as titanium content increased, ferrite percentages rose and pearlite percentages fell. However, the hardness profile of welded parts did not follow a predictable pattern as titanium content was increased. Before mixing TiO_2 powder in commercial granular flux, examine hardness, bead shape, and grain size. Use of TiO_2 powder combined with commercial flux; welding conditions remain constant. TiO_2's effect on Submerged Arc Welding weld metal was compared with the results to determine an optimal ratio.

Keywords: Titanium dioxide powder; flux; bead geometry; grain size; hardness; microstructure; SAW.

INTRODUCTION

Fluxes influence the metal's chemistry in submerged arc welding (SAW). The weld's mechanical properties are determined by WM microstructure. Ti, Ni, B, Mo, Cr, etc. are key microstructure components. Welding consumables can improve weld quality. WM makeup has been altered in previous experiments [1–2]. Use of additional fluxes and modifying the WM's chemical composition with filler or metal powder are two ways to improve its properties. For welding, AF's fine grain size, low dislocation density, and delayed crack propagation are ideal. Several oxides, including titanium, zirconium, and boron, can boost SAW AF output. Flux oxides can dissolve oxygen and metal when welding [3–4]. By adding titanium and boron at modest concentrations, the SAW process produced more AF. A lot of titanium promotes strain hardening and subsequent phases. The microstructure and chemical composition of HSLA steel non-metallic inclusions are affected by the elements titanium, nickel, molybdenum, and chromium. The microstructural development of WM is unaffected by titanium concentrations between 50 and 400 ppm [5–6]. The microstructure of WM is regulated by inclusions made of materials other than metal. Grain boundaries in austenite may become pinned by inclusions, causing the grains to become smaller. High-strength, low-alloy welds may have a reduced fracture resistance if these inclusions are present [7–8]. Heterogeneous AF nucleation is

***Author for Correspondence**
Rishabh Chaturvedi
E-mail: rishabh.chaturvedi@gla.ac.in

[1,2]Assistant Professor, Department of Mechanical Engineering, GLA University, Mathura, Uttar Pradesh, India

Received Date: December 12, 2022
Accepted Date: September 01, 2023
Published Date: September 10, 2023

Citation: Rishabh Chaturvedi, Aman Sharma. TiO_2 Refined Flux Provides Significant Impact on Saw Bead Shape, Particle Size, and Hardness. Journal of Polymer & Composites. 2023; 11(Special Issue 4): S70–S80.

encouraged by the presence of Ti-containing inclusions, the density of which grows in proportion to the amount of Ti flux. Elongation and impact strength improve whereas yield, UTS, and Vickers hardness decrease with increasing Ti concentration. As a result of Ti addition, the microstructure and inclusion formation of pipeline steel are modified. Small amounts of bainite (B) and ferrite with M/A microconstituents are formed in WM as the Ti level rises [9–10]. TiO_2 increases the toughness of welds to impact, but it also makes them more vulnerable to cracking due to hydrogen (HIC). The amount of aluminium in WM has an effect on the chemical makeup of the inclusions, which in turn encourages ferrite nucleation. The mechanical properties of WM can be affected by its grain structure. The resistance to damage inflicted by a Charpy V-notch drops in tandem with the tensile strength of WM steel. There are two upsides to having fine equiaxed grains in the fusion zone [11–12]. As a first step, WM with fine granules is less likely to crack during welding. Steels and stainless steels can benefit from fine grains that increase ductility and fracture toughness in the resulting weld. Grain has therefore been improved in the weld fusion zone. In order to perform SAW on mild steel, titanium carbide and ferrotitanium-titanium carbide mixes were introduced as inoculant powders into the weld pool. During manual metal arc welding, ferritic high strength steel responds differently depending on whether or not the molybdenum (Mo) powder coating has been altered. In WM, the columnar microstructure was refined as Mo and Mn concentrations. Tibor was added to 7108 aluminium castings and gas tungsten arc welds, and the effect on grain refinement and solidification was evaluated [13–18]. In the case of alloy 7108, The same amount of tibor was able to refine grains to a finer consistency than the same amount of scandium. Due to its high affinity for oxygen and sulfur, zirconium improves the hardness and cold work qualities of steel. It turns out that the aforementioned investigation reveals a plethora of studies on the incorporation of titanium into structural steels. Effects of Ti enrichment on bead morphology and grain refinement are not well understood. Submerged arc weld beads are examined for their geometry, grain size, and hardness, as well as the effect of titanium dioxide in fluxes [19–21].

Specification of SMAW Welding

SMAW, also known as flux shielded arc welding, stick welding, or manual metal arc welding (MMA or MMAW), involves coating a consumable electrode in flux. A welding power source supplies direct or alternating current to an electrode, creating an electric arc between it and the metals to be welded. "Weld pools" occur when the workpiece and electrode melt together. As the weld is placed, the flux coating on the electrode degrades, releasing shielding vapours and creating a layer of slag that protects the weld area. Shielded metal arc welding is one of the oldest and most widely utilised types of welding it is also one of the most versatile and simple to operate. Additionally, it is a widely used approach. Even though flux-cored arc welding is becoming more common, shielded metal arc welding, often known as SMAW, is still used in major steel constructions and industrial fabrication. Figure 1 shows the SMAW configuration.

Figure 1. Setup SMAW Welding.

Material Used

TiO_2 Powder

Titanium dioxide form rutile (TiO_2) Although most titanium dioxide is made from ilmenite; rutile is an economically significant titanium mineral. Figure 2 shows TiO_2 powdered form, it creates brownish-red crystals, frequently in twins or rosettes. Switzerland, Norway, Brazil, and the U.S. have the most rutile. Iron oxide, chromium oxide, and vanadium oxide contain rutile [22–23]. Rutile has 4/mm 2/mm 2/mm tetrahedral symmetry. Parallel chains of octahedrons, each with a titanium ion and six oxygen atoms, make up its structure. The model below shows octahedron edges and base structure. Synthetic rutile can be colored by doping, although pure material is colorless. High refractive index produces diamond-like luster and strong refraction. Titania is a near-colorless diamond replacement. Rutile is soft and rarely used in jewelry (scratch-resistant).

Low Alloy Steel Plate

Welding and fabricating problems arise with low-alloy steels. How well an alloy steel welds depends on the specific alloy steel and the intended use. The problem of weldability is complicated by the fact that every alloy combination presents its own challenges. There isn't a magic bullet that'll work for everyone. After welding, it is necessary to have a thorough understanding of the metallurgical structures of each of these categories, including the modified variations. This needs careful consideration and following preheat, interphase, and PWHT. 9% chromium and molybdenum steel is used to make industrial heat exchangers. Successful welds require a well-developed welding method and heat control procedures to prevent steel phase development. In process facilities, low alloy steels with less than 0.2% carbon and 12% alloying elements are useful (Ni, Cr, Mo, V, B, W, or Cu). Manufacturers normalize and temper many low-alloy steels, but quenching and tempering is becoming more popular. Some low alloy steels require pre- or post-weld heat treatment to prevent weld zone cracking. Figure 3 Shows Low alloy steel plates

Figure 2. TiO_2 powdered form.

Figure 3. Low alloy steel plates.

EXPERIMENTAL SETUP AND PROCEDURE

By varying the amount of TiO_2 powder added to the flux, the chemical makeup of WMs can be changed, and the filler wire used remains constant. Amounts of TiO_2 metal powder (2.5, 5, 7.5, 10, and 12.5%) were manually blended with commercial fluxes. TiO_2 could not be added past the maximum because welding (visual inspection) was subpar and slag detachability was low after that point. In all welding situations, the process parameters were the same. It was compared to newly purchased commercial flux welds. A plate made of low alloy steel with a thickness of 16 mm was utilised in this experiment. Table 1 contains a breakdown, in terms of weight percent, of the chemical components that make up the electrode wire and the base plate. The copper-coated electrode that was used (AWS A/S 5.17: EH 14) has a diameter of 4 mm and was employed. In order to complete the welding process, we utilised a fused silicon product known as AUTOMELT A55. (grain size ranging from 0.2 to 1.6 mm; basicity index of 1.6) The parameters of the welding process that are stated in Table 2 are appropriate in most situations. For the purpose of this experiment, the data from six separate pieces of welded low alloy steel plates will be blended together.

Table 1. Base plate and electrode wire chemical composition (by weight, in percent)

Element	Manganese	Carbon	Sulphur	Phosphorus	Silicon	Carbon eq
Electrode	0.4	0.04	-	-	0.05	-
Base plate	0.419	0.163	0.013	0.019	0.150	0.24

Table 2. Process parameter for welding

Specimen No.	Percentage (%) of TiO_2	feed rate of wire (mm/min)	Basicity index	Traverse speed (m/min)	Current (A)	Voltage (V)	Stickout (mm)
1	0	160	1.6	0.75	750	38	25
2	2.5	160	1.52	0.75	750	38	25
3	5	160	1.44	0.75	750	38	25
4	7.5	160	1.37	0.75	750	38	25
5	10	160	1.31	0.75	750	38	25
6	12.5	160	1.24	0.75	750	38	25

When all testing was complete, the test plates were inspected visually and using ultrasound technology for weld flaws. In order to cut test specimens transverse to the welding direction, a hydraulic power saw was used to automatically slice pieces of material 12–15 mm wide. For the purpose of metallographic examination, welded specimens were first polished using emery paper with successively finer grits, and then they were finished with a layer of diamond paste. Slightly etched samples showed weld zones after being polished. We utilised an optical microscope and image analysis software to determine the exact dimensions of the grains and the geometrical make-up of the beads. Linear-intercept methods are used to determine particle sizes in accordance with ASTM E112. Inclusion analysis made use of SEM and EDX. The weld was put through its paces in a Vickers microhardness machine, which applied a 2 kg load steadily for 10 seconds. Figure 4 shows the SMAW weld specimen

OUTCOMES AND EXPLANATION

Chemical Composition of WM

Following the addition of TiO_2 powder to the flux, the elemental composition of the WM changed. In Table 3, find the findings from our analysis of the chemical make-up of all weld metals. Aside from titanium, which showed a systematic range of 0.01%-0.03%, all of the other results were reasonably consistent.

TiO_2's Impact on Weld Bead Formation

TiO_2-infused weld beads deviated in shape from those produced by commercial flux. Macrographs of weldment are displayed in Figure 5 for TiO_2 additions of 4% and 12%. TiO_2 enriched flux welding

produced weld pools that were narrower and deeper. TiO_2 impact on reinforcing, bead width, and penetration depth. Figure 6 depicts the reaction (R). Up to a TiO_2 level of 10%, P rises progressively, but then begins to decline. In comparison to the WM that has just been refreshed, P goes up by around 20%. W falls by up to 5% when combined with TiO_2 then rises again.

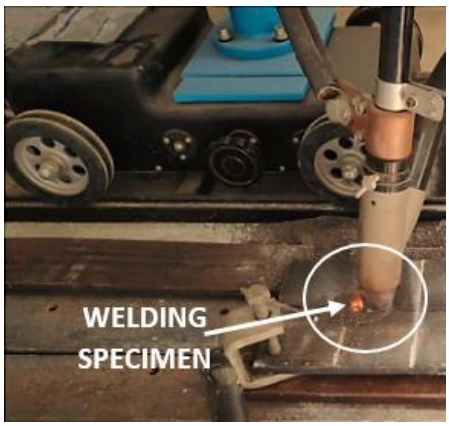

Figure 4. SMAW Weld Specimen.

Table 3. Welding Metal Constituents

Element	Ti	Si	C	P	Mn	S
WM-T0	0.01	0.312	0.102	0.018	0.94	0.0099
WM-T 2.5	0.016	0.311	0.104	0.02	0.94	0.010
WM-T 5	0.017	0.310	0.101	0.019	0.90	0.0098
WM-T 7.5	0.02	0.298	0.104	0.020	0.91	0.010
WM-T 10	0.027	0.296	0.102	0.021	0.89	0.010
WM-T 12.5	0.030	0.291	0.103	0.02	0.89	0.011

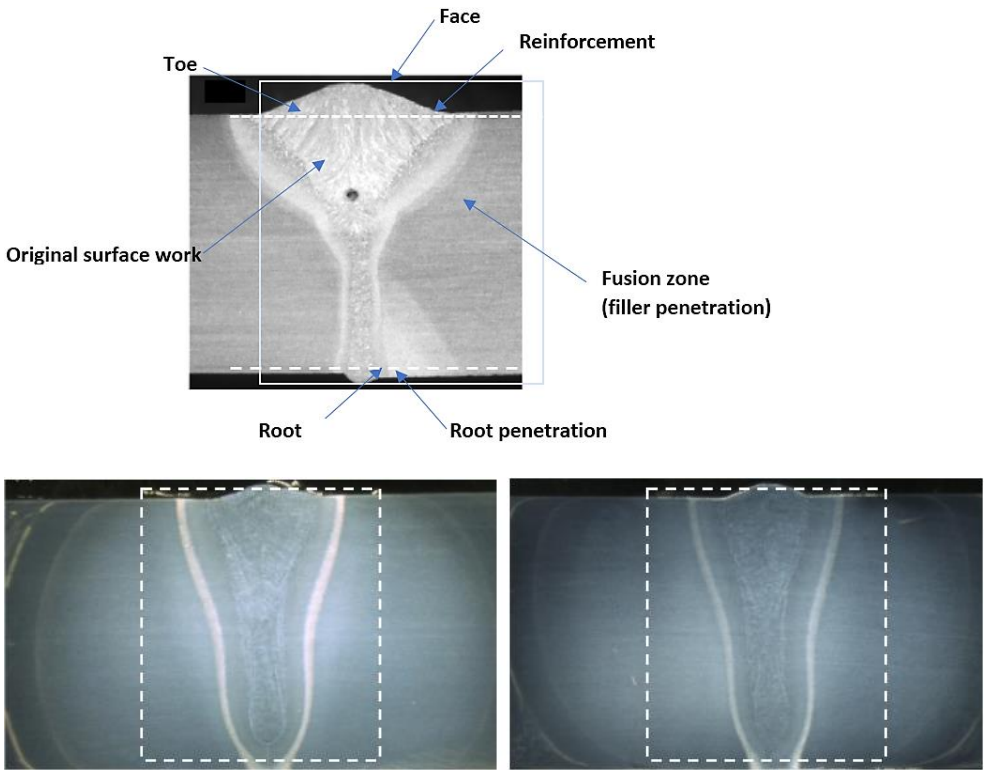

Figure 5. Weld bead at TiO_2 4% and 12%.

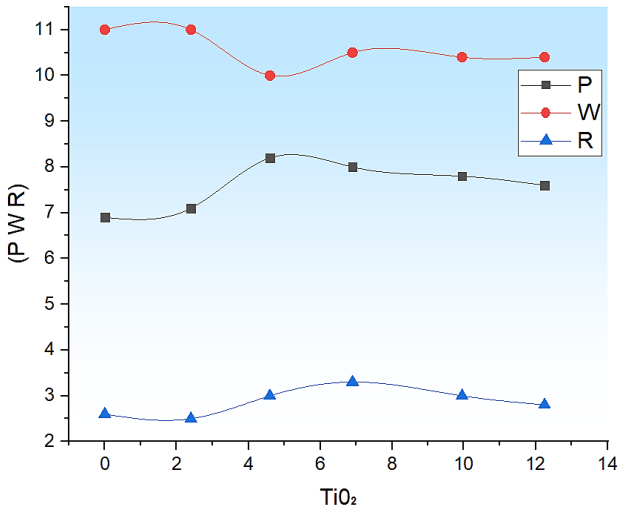

Figure 6. TiO_2's impact on the parameters of the bead geometry.

Figure 6. shows TiO_2's impact on the parameters of the bead geometry. When compared to a completely new flux weld, W drops in every scenario. TiO_2 has little impact on R. With enhanced fluxes, R marginally rises. R is proportional to metal deposition; when traverse velocity falls, R values rise. Since the welding circumstances are now the same for everyone, there is no longer a discernible relationship between R and the enriched fluxes. Because oxides grow with enhanced flow, P rises along with TiO_2 concentration. It is the oxygen concentration in the TiO_2 enriched fluxes that is responsible for the enhancement of P. In this case, oxygen is employed as a surface-active ingredient, and consequently, Marangoni convection is inverted. The bead's shape is determined by heat sources and Marangoni convection above the weld pool. As temperature increases, surface tension is lost in pure metals and alloys. Weld pools' surface tension is impacted by the significant temperature difference between their centre and edges. When the arc is in place, fluid will migrate from the middle of the pool to the edge, where the surface tension will be higher since the temperature will be lower. Because heat is easily transferred from the centre to the periphery, the weld that is produced is wide but not particularly deep. Figure 7 uses the Marangoni model to illustrate the flow of the process.

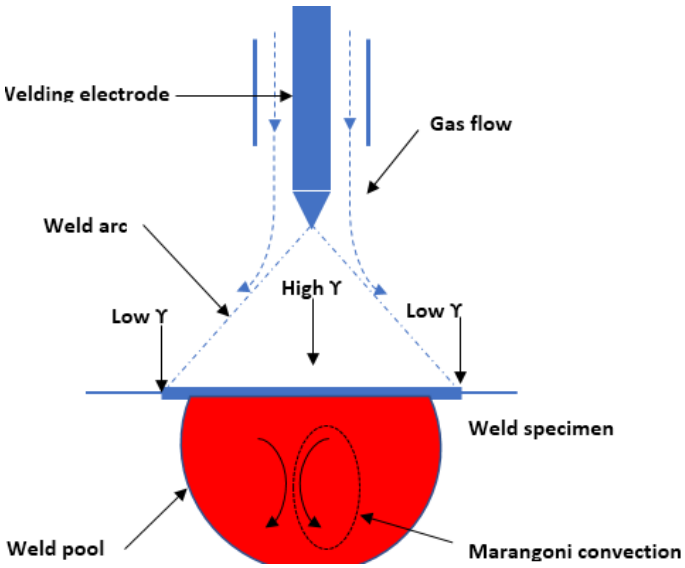

Figure 7. Flow based on the Marangoni model.

When the concentration of surface-active components such as sulfur, oxygen, or selenium in a stainless-steel weld pool changes, one can observe a change in the direction of the Marangoni

convection that is occurring in the weld pool. WM rises over a critical amount. A narrow, but deep, weld was used here. For enrichments more than 10% TiO_2, P marginally decreases. This could be because of the WM's increased TiO_2 concentration. A high concentration of titanium dioxide (TiO_2) in the flux prevents it from breaking down completely, leaving behind solid oxide particles that float on the water's surface. As the percentage of TiO_2 in the bead geometry rises in comparison to commercial flux, its overall appeal rises as well. P and W demonstrating the enhanced bead shape for maximum stringing efficiency.

TiO_2's Effects on the Microstructure and Grain Size of WM

In Figure 8 micrographs of the weld zones after being subjected to various welding settings. Microstructural variations in WMs as a function of alloying element concentration are investigated. Microconstituents such as pearlite, B, and M/A were also found in the WM's microstructure with AF, GBF, WF, and other phases. It is clear that when titanium concentration rises, the proportion of AF rises as well, whereas the percentages of the other ferrites fall. When there is a higher percentage of titanium in the flux, the average length of the AF is shorter. Titanium is a valuable material for generating carbide and nitride, according to the research that is currently available in the literature. Because of the way that they align so well with ferrite planes, TiN and TiC particles make for ideal AF nucleation sites. Ferrite crystallises from austenite because of the disparity between their chemical free energies and the system's inclination to reduce interface barrier interfacial free energy. This also plays a role in the process.

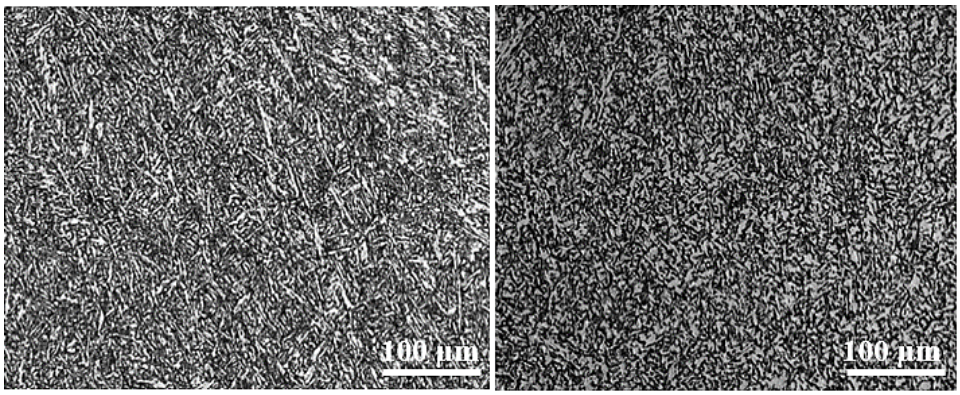

Figure 8. Micrographs of welded metal under various welding situations.

Deoxidation and/or desulfurization in the weld pool created non-metallic impurities in this work. According to certain research, by acting as AF nuclei, these inclusions are critical to the microstructural evolution of ferritic WMs. Additionally, it has been proposed that inclusions may function as pins and cause the austenite grain size to decrease. The EDX results for WM inclusion are displayed in Figure 9. The incorporation of Ti into inclusions facilitates the growth of AF. The amount of Mn and Si in the inclusions decreases as the weld's Ti content rises, as the weld's Ti content rises, and so on. As can be seen in Figure 10, ferrite and pearlite both make up a small fraction of WMs. A higher percentage of ferrite and a lower pearlite percentage can be expected when TiO_2 is added to the flux.

A characteristic lamellar ferritic and pearlitic microstructure may be seen in the base metal used in this work. At low magnification, the micrograph reveals that the little carbide particles are not visible among the darkly etched pearlite and lightly etched ferrite phases. The percentage of ferrite in the WM increases from 38.8 to 56 percent, while the percentage of pearlitic drops from 62.6 to 56 percent, as a result of an increase in titanium in the WM. It is evident from the fact that the addition of titanium dioxide increases AF nucleation. the typical breadth of pearlite and ferrite at various TiO_2 contents. Figure 10 makes it very evident that TiO_2 additions aid in the WM's grain refining. The mean grain size of ferrite and pearlite is smaller than it would have been with industrial flux welding.

According to earlier research, solute components influence the refinement of grains by regulating the growth of the nucleated grains. The issue of growth constraints can help explain the phenomenon (GRF). Where k is the coefficient for converting a liquid into a solid and m is the liquidus gradient, C0 is the bulk composition, Grain growth is slowed because alloying elements diffuse slowly due to the constitution undercooling caused by the elements.

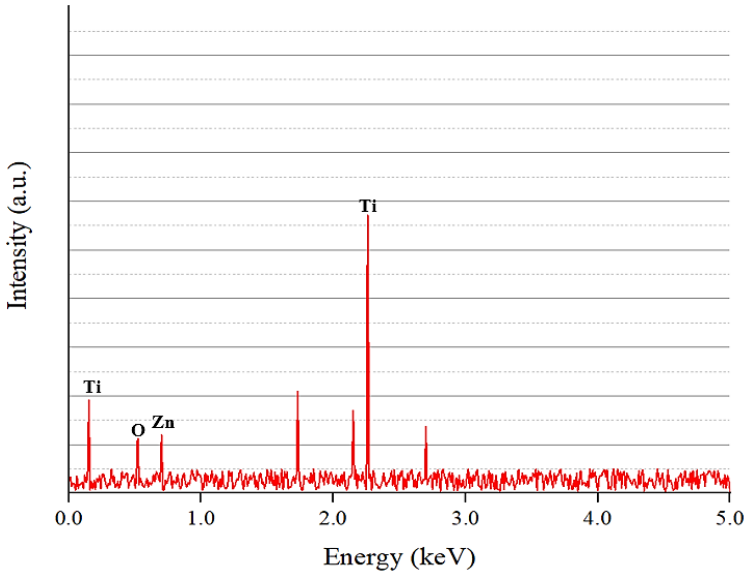

Figure 9. Weld metal inclusion EDX analysis.

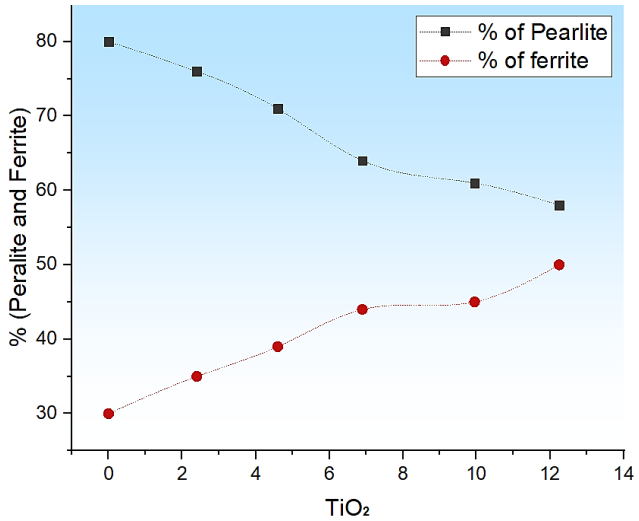

Figure 10. TiO_2 content% of ferrite and pearlite.

Since the titanium content in the WM increases at a slower rate than the diffusion of the solute, the rate of crystal formation is slowed and the grain size is refined as the solid/liquid boundary approaches, leading to a higher constitutional undercooling.

TIO_2'S IMPACT ON HARDNESS

Figure 11 depicts the weldment's hardness profile under various welding conditions. Titanium oxide's effect on the material's hardness is inconsistent. The addition of 2.5%-7.5% TiO_2 caused a drop in hardness, followed by an increase. The drop in hardness and the corresponding decrease in pearlite% with titanium content appear to be attributable to the pearlite% in WM. Increases in TiO_2 content lead to a rise in hardness, from 165.3 to 210.6. This may explain why the hardness of WM

with a greater amount of titanium added has a microstructure dominated by TiC and TiN. There is no correlation between the hardness of WM and its titanium content, either, according to the research. Hardness levels in the weld metal (WM) were consistent across all sections, however values dropped as the test went through from fusion line to substance, HAZ is the region where heat damage has occurred. When looking at the HAZ hardness curve, coarse grain HAZ is where it peaks, whereas fine grain HAZ is where it dips. The base material was determined to be the softest component.

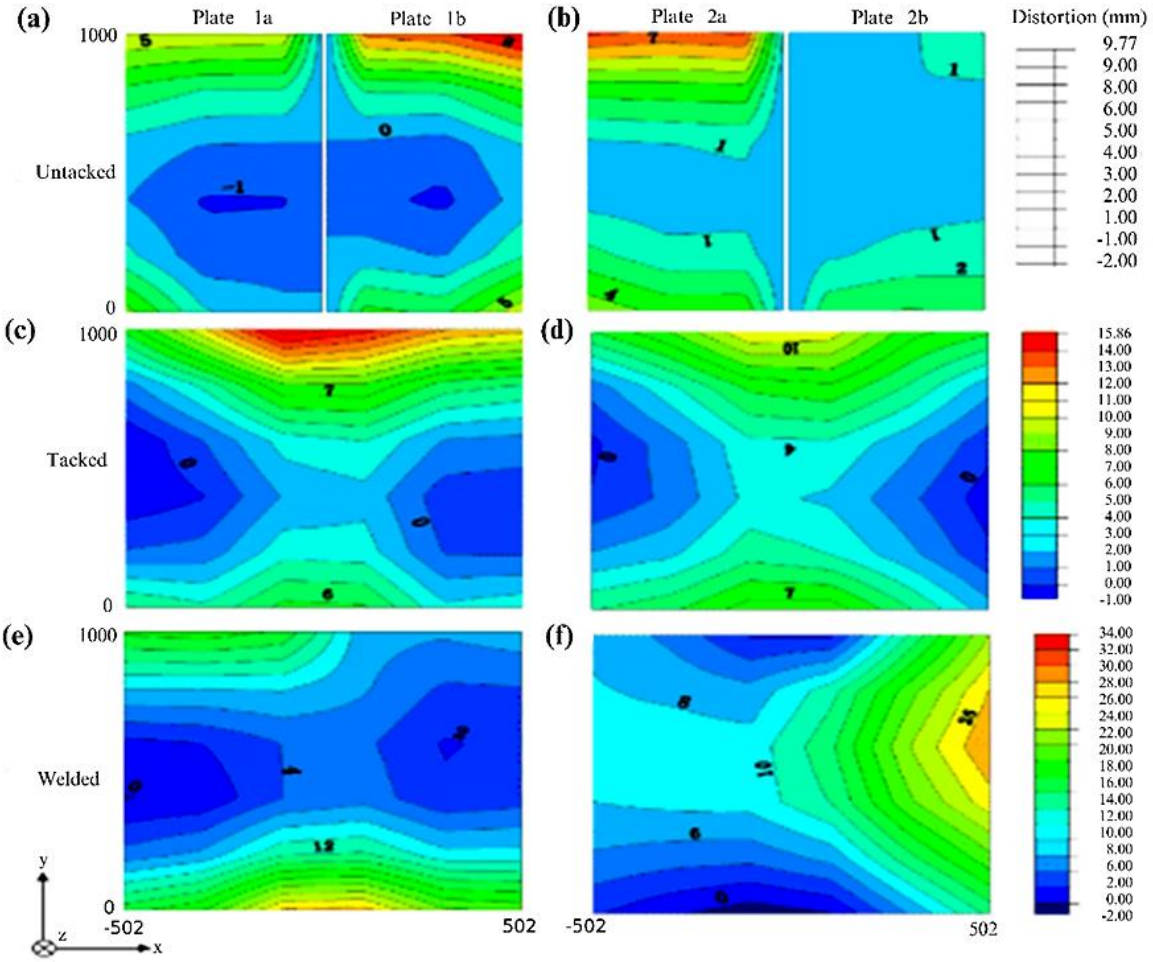

Figure 11. TiO_2 weld metal hardness distribution.

CONCLUSION

Investigations have been done on the relationship between the amount of TiO_2 powder supplied to the flux and low alloy steel WMs' bead shape hardness and grain size. The quantity of titanium oxide powder used was discovered to be a factor in these results. Based on findings of that investigation, we are able to draw the following conclusions:

- Titanium oxide was added to the flux, which resulted in the beads taking on a different form. P increases considerably with increasing titanium content but decreases as it reaches maximum TiO_2 concentration. When the concentration of titanium is increased, it is possible to create beads with geometries that are more aesthetically fair.
- WMs optical micrographs show a ferritic and pearlitic microstructure that is more evenly spread than commercial flux welding, which enhances the response properties all around. Content of titanium affects AF formation. In the process of analysing the phases of WMs, it was discovered that the percentage of ferrite rises while the percentage of pearlite falls. A smaller grain size of the ferrite and pearlite in WMs can be achieved by using titanium in the flux

- The addition of TiO_2 to WMs does not result in the emergence of any discernible pattern, and the hardness value of WMs is not altered in any way. However, due of the presence of harder phases, the value of the material's hardness increases in proportion to the increasing titanium content. According to the research that was discussed previously, adding TiO_2 powder during SAW has the potential to improve the grain size refinement, hardness, and weld bead.

REFERENCE

1. Babu NK, Talari MK, Dayou P, Zheng S, Jun W, SivaPrasad K. Influence of titanium–boron additions on grain refinement of AA6082 gas tungsten arc welds. Materials & Design. 2012 Sep 1;40: 467–75.
2. Beidokhti B, Koukabi AH, Dolati A. Effect of titanium addition on the microstructure and inclusion formation in submerged arc welded HSLA pipeline steel. Journal of Materials Processing Technology. 2009 Apr 21;209(8):4027–35.
3. Beidokhti B, Koukabi AH, Dolati A. Influences of titanium and manganese on high strength low alloy SAW weld metal properties. Materials Characterization. 2009 Mar 1;60(3):225–33.
4. Muzamil M, Wu J, Akhtar M, Patel V, Majeed A, Yang J. Multicomponent enabled MWCNTs-TiO2 nano-activating flux for controlling the geometrical behavior of modified TIG welding joint process. Diamond and Related Materials. 2019 Aug 1;97:107442.
5. Saini S, Singh K. Recycling of steel slag as a flux for submerged arc welding and its effects on chemistry and performance of welds. The International Journal of Advanced Manufacturing Technology. 2021 May;114(3):1165–77.
6. Bose-Filho WW, Carvalho AL, Strangwood M. Effects of alloying elements on the microstructure and inclusion formation in HSLA multipass welds. Materials characterization. 2007 Jan 1;58(1):29–39.
7. Kumar A, Sharma K, Dixit AR. A review of the mechanical and thermal properties of graphene and its hybrid polymer nanocomposites for structural applications. Journal of materials science. 2019 Apr;54(8):5992–6026.
8. Wang Z, Zheng X, Zhong M, Li Z, Wang C. Crystallization behavior of CaF2-TiO2 fluxes geared towards high heat input submerged arc welding. Journal of Non-Crystalline Solids. 2022 Sep 1;591:121716.
9. Kumar M, Pilania V, Kumar G, Chandra R. Effect of adding different powders in saw agglomerated flux on the mechanical properties of 1025 welds. IAETSD Journal for Advanced Research in Applied Sciences. 2018;5(5):158–67.
10. Sharma L, Chhibber R. Design and development of submerged arc welding fluxes using TiO2-SiO2-CaO and SiO2-CaO-Al2O3 flux system. Proceedings of the Institution of Mechanical Engineers, Part E: Journal of Process Mechanical Engineering. 2019 Aug;233(4):739–62.
11. Fattahi M, Nabhani N, Hosseini M, Arabian N, Rahimi E. Effect of Ti-containing inclusions on the nucleation of acicular ferrite and mechanical properties of multipass weld metals. Micron. 2013 Feb 1;45:107–14.
12. Chaturvedi R, Islam A, Sharma K. A review on the applications of PCM in thermal storage of solar energy. Materials Today: Proceedings. 2021 Jan 1;43:293–7.
13. Ragavendran M, Vasudevan M, Hussain N. Study of the Microstructure, Mechanical Properties, Residual Stresses, and Distortion in Type 316LN Stainless Steel Medium Thickness Plate Weld Joints. Journal of Materials Engineering and Performance. 2022 Jan 21:1–3.
14. Kolhe KP, Datta CK. Prediction of microstructure and mechanical properties of multipass SAW. Journal of materials processing technology. 2008 Feb 1;197(1–3):241–9.
15. Lu S, Fujii H, Nogi K. Marangoni convection and weld shape variations in Ar–O2 and Ar–CO2 shielded GTA welding. Materials science and engineering: A. 2004 Aug 25;380(1–2):290–7.
16. Xie F, Shen J, Song H, Xie X. Effects of cerium and SiC mixed particles on nanoparticle strengthening activated TIG-welded AZ31 alloy joints. Journal of Materials Research. 2018 Dec;33(24):4340–8.

17. Sharma A, Chaturvedi R, Sharma K, Saraswat M. Force evaluation and machining parameter optimization in milling of aluminium burr composite based on response surface method. Advances in Materials and Processing Technologies. 2022 Feb 20:1–22.
18. Vora J, Patel VK, Srinivasan S, Chaudhari R, Pimenov DY, Giasin K, Sharma S. Optimization of activated tungsten inert gas welding process parameters using heat transfer search algorithm: with experimental validation using case studies. Metals. 2021 Jun 19;11(6):981.
19. Paniagua-Mercado AM, López-Hirata VM, Muñoz ML. Influence of the chemical composition of flux on the microstructure and tensile properties of submerged-arc welds. Journal of Materials Processing Technology. 2005 Dec 1;169(3):346–51.
20. Paniagua-Mercado AM, Lopez-Hirata VM, Dorantes-Rosales HJ, Diaz PE, Valdez ED. Effect of TiO2-containing fluxes on the mechanical properties and microstructure in submerged-arc weld steels. Materials Characterization. 2009 Jan 1;60(1):36–9.
21. Prasad K, Dwivedi DK. Some investigations on microstructure and mechanical properties of submerged arc welded HSLA steel joints. The international journal of advanced manufacturing technology. 2008 Mar;36(5):475–83.
22. Trindade VB, Mello RS, Payao JC, Paranhos RP. Influence of zirconium on microstructure and toughness of low-alloy steel weld metals. Journal of materials engineering and performance. 2006 Jun;15(3):284–6.
23. AlIthari AS, Thahab SM, Al-Obbaidi AF. Effect of adding TiO2 nanoparticles on the impact toughness for welding joints of mild steel. Australian Journal of Mechanical Engineering. 2020 Sep 25:1–4.

